ELSEVIER

Neurocomputing 38–40 (2001) 129–139

NEUROCOMPUTING

www.elsevier.com/locate/neucom

Simple models of bursting and non-bursting P-type electroreceptors

Maurice J. Chacron[a,*], André Longtin[a], Leonard Maler[b]

[a]*Physics Department, University of Ottawa, 150 Louis Pasteur, Ottawa, Ont., Canada K1N-6N5*
[b]*Department of Cellular and Molecular Anatomy, University of Ottawa, 451 Smyth Rd., Ottawa, Ont., Canada K1H-8M5*

Abstract

Weakly electric fish use phase and amplitude modulations of their electric organ discharge to communicate and to capture prey (electrolocation). P-type electroreceptors, also known as probability coders, on their skin can detect extremely weak signals. We analyse baseline firing characteristics of these receptors from experimental data, and present mathematical models for the firing activity of both bursting and non-bursting units.

Keywords: Electroreceptor, Electrolocation, Interspike interval analysis, Weak signal detection, Correlations

1. Introduction

Weakly electric fish generate an electric field through their electric organ discharge (EOD) in order to communicate and detect prey. Nearby objects with a conductivity different than that of surrounding water cause distortions in the field; the ensuing electric field amplitude modulations (AMs) change the potential across the fish's skin. Highly sensitive P-type electroreceptors encode these modulations into trains of action potentials to be analyzed by the higher brain centers (see [11,15] for a review).

* Corresponding author. Tel.: + 1-613-562-5800 ext. 8096; fax: + 1-613-562-5190.
E-mail address: mchacron@physics.uottawa.ca (M.J. Chacron).

0925-2312/01/$ - see front matter
PII: S0925-2312(01)00549-5

The unit consists of 25–40 receptor cells and a nerve fiber that makes synaptic contact to at least 16 active neurotransmitter release sites per receptor cell [2]. Although intra-cellular recordings are not yet possible on such cells, spikes can be recorded from their axons (see e.g. [14]). We are interested in the activity of P-units in the gymnotiform species *Apteronotus Leptorhynchus* (Brown Ghost Knife Fish). Their EOD is sinusoidal in nature (frequency 600–1200 Hz) and acts as a carrier signal for AMs caused by nearby objects [1]. Some models have already been proposed [10,7]. The lack of experimental data makes parameter estimation for detailed models [7] very difficult. Further, even though the detailed model in [7] reproduces tuning curve data, it does not display the pattern of skipped phase locked firings seen experimentally. The model in [10] accounts for the linear properties of AM coding; however, it has no firing dynamics and does not include refractory effects. A recent model [3] of the firing dynamics successfully accounts for the baseline firing interval distribution and correlations.

From detailed analysis of the available experimental data (Section 2), we present a modified version of the model in [3] for non-bursting afferents (Section 3). We further show how an extended version of our model can lead to bursting behavior observed experimentally in certain P-units (Section 4).

2. Experimental data

P-type electroreceptors have been classified into two groups: Bursters (B) and non-bursters (NB) [14]. We show in Figs. 1 and 2 data obtained for both types when no stimulus is applied (i.e. when the receptor is only driven by the EOD of the fish without modulations) (data courtesy of Mark Nelson, Beckmann Institute, Illinois, USA).

One can see that the interspike interval histograms (Figs. 1a and 2a) (ISIHs) show Gaussian shaped modes at multiples of the EOD period in both cases; this is seen because the unit skips a random number of EOD cycles between each action potential. Furthermore, each unit can fire at most once per EOD cycle. This implies that the afferent's firings are phase-locked [4] to the EOD signal and that there is at most once spike per EOD cycle. For NB units, the ISIH envelope is approximately Gaussian. In addition to this, B units show a very prominent mode at 1 EOD period which implies that when an action potentials is fired, it is followed by one or more firings on the next EOD cycles followed by a period of quiescence. This results in a bursting pattern.

The return maps (Figs. 1b and 2b) show clusters centered at integer multiples of the EOD period as expected from phase-locking. Furthermore, the negatively sloped elongation observed in both cases is also a signature of phase-locking [8]. This implies that if a firing leads/lags the mean EOD phase, then on average the next firing will lag/lead the mean EOD phase so that the firings keep in step with the EOD.

Finally, we see (Figs. 1c and 2c) that both units exhibit negative serial correlation coefficients (SCC) at low lags. These are expected from refractory effects at such high

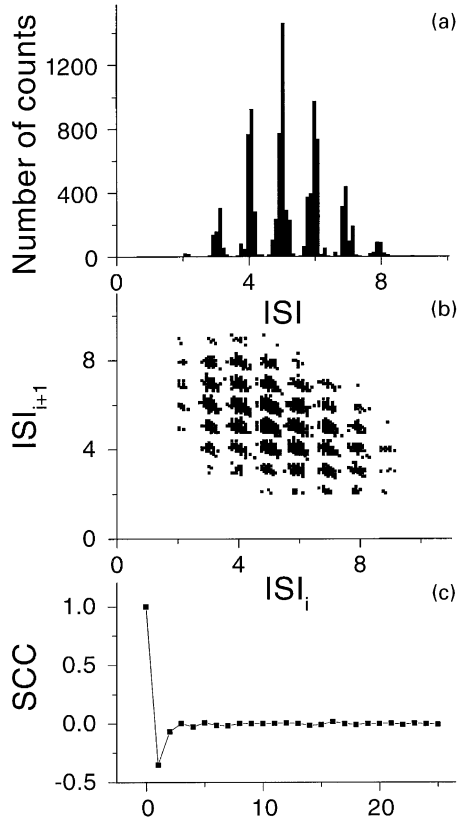

Fig. 1. Experimental data consisting of 10 000 consecutive interspike intervals from a non-bursty unit (courtesy of Mark Nelson, Beckmann Institute, Illinois, USA). Time is in EOD cycles; the EOD frequency was 755 Hz. (a) ISIH, (b) return map, (c) serial correlation.

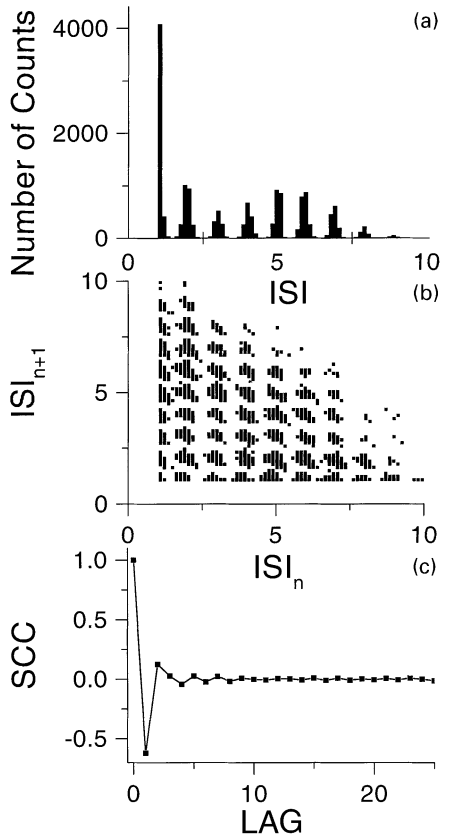

Fig. 2. Experimental data consisting of 10 000 consecutive interspike intervals from a bursty unit (courtesy of Mark Nelson, Beckmann Institute, Illinois, USA). 10 000 ISIs were analysed. Time is in EOD cycles, the EOD frequency was 850 Hz. (a) ISIH, (b) return map, (c) serial correlation.

firing rates [5,12]. As mentioned above, intra-cellular recordings are not yet possible for such cells. However, there are a number of plausible physiological mechanisms that could account for this refractoriness. They include: slow sodium cumulative inactivation [9], synaptic desensitization [6], or other slow negative adaptation currents [13].

Models must thus reproduce the following features of experimental data: phase-locking with random skipping to sinusoidal input, as well as relative refractoriness that persists for several EOD cycles.

3. The model

We start with the leaky integrate and fire (LIF) model [12] described by the equation

$$\dot{V} = -\frac{V}{\tau_v} + \frac{I_{syn}}{C}, \tag{1}$$

where V is the membrane potential, τ_v is the membrane time constant and C is the capacitance (we set $C = 1$). When V reaches a constant threshold θ, it is reset to zero and a spike is said to have occurred. It is important to note that such a model is memoryless in the sense that ISIs are uncorrelated when driven by periodic input and/or white noise.

We note that all the aforementioned mechanisms that could account for the relative refractoriness seen experimentally lead to an increase in the effective voltage-threshold distance. We thus choose as in [3] to make the threshold a dynamical variable governed by

$$\dot{\theta} = (\theta_0 - \theta)/\tau_\theta, \tag{2}$$

where θ_0 is an equilibrium value towards which θ relaxes exponentially with time constant τ_θ. When V equals θ, it is reset to zero as in the standard LIF model while θ is incremented by a fixed amount $\Delta\theta$ to simulate refractoriness. Furthermore, V is kept constant for the duration of the absolute refractory period T_r. We thus have a leaky integrate-and-fire with dynamic threshold (LIFDT) model. We note that relative refractoriness can be modeled in other ways. For example, one could model this using voltage hyperpolarisation as in [5] or through negative adaptation currents [13].

Finally, we hypothesize periodic input in the form of a rectified sine wave [3]:

$$I_{syn} = A\sin(2\pi ft)H(\sin(2\pi ft))\,(1 + OU_1) + OU_2, \tag{3}$$

where H is the Heaviside function to account for rectification while A is the EOD amplitude and f is the EOD frequency. To account for variability seen in the spike train, we add synaptic noise in the form of two Ornstein–Uhlenbeck (OU) processes OU_1 and OU_2 with zero mean and variances D_1/τ_{OU1} and D_2/τ_{OU2}. This is different from [3] where OU_1 was replaced by Gaussian white noise that is constant over one EOD cycle. Our results here (see below) also agree with data; thus our stochastic dynamical model does not depend sensitively on the correlation time of the noise process OU_1, as long as it can be considered "fast" as compared to the model dynamics.

We show in Fig. 3a the deterministic dynamics ($D_1 = D_2 = 0$) obtained with the model. Parameters have been adjusted so that 5:1 (1 spike every 5 EOD cycles) periodic firing occurs ($I_i = I_{i+1}$); this is clearly a suprathreshold forcing regime. In the stochastic case (Fig. 3b), we see that we have a phase-locked skipping pattern. Let us denote by θ_s the mean value of θ immediately after a spike. We see that if an ISI is shorter than average (I_i in Fig. 3b), then θ after the spike that ends I_i is greater than θ_s, consequently the next ISI (I_{i+1}) will have a greater probability of being longer than average since θ will take longer to decay to equilibrium. The converse statement is

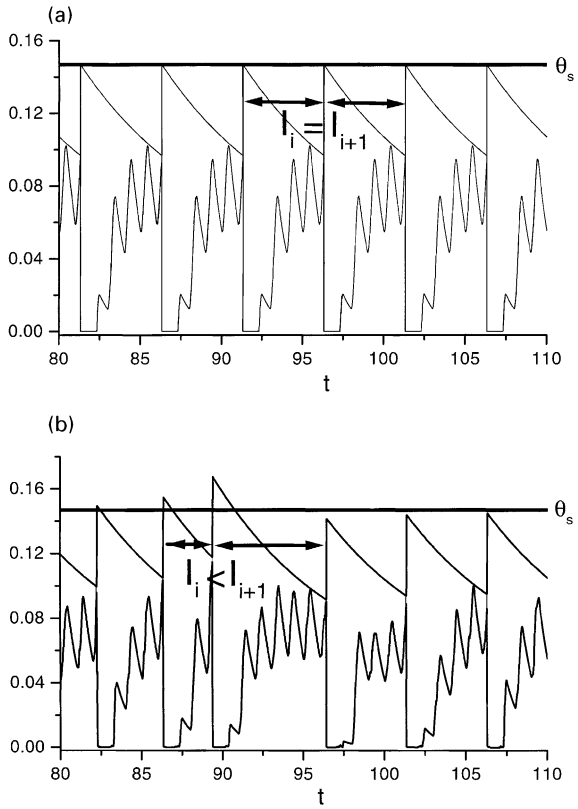

Fig. 3. Voltage (lower curve) and threshold (upper curve) trace obtained with the model (Eqs. (1)–(3)). (a) without noise, (b) with noise. Parameters are (time is in EOD cycles): $dt = 0.0025$, $T_r = 1, f = 1000$ Hz, $A = 0.2613$, $\theta_0 = 0.04$, $\Delta\theta = 0.05$, $\tau_v = 1$, $\tau_\theta = 8.5$, $D_1 = 8$, $\tau_{OU1} = 0.025$, $\tau_{OU2} = 0.075$, $D_2 = 0$.

also true. This mimicks cumulative refractoriness and thus gives rise to a negative serial correlation coefficient (SCC) at lag one. Note that the relative refractoriness is deterministic in nature because the threshold carries the memory. However, without noise to perturb the 5:1 periodic pattern, the negative correlations carried by this memory would not be revealed.

We now show results obtained with the model for physiologically realistic parameters in Fig. 4. Comparing with the data in Fig. 1, we see that the main features are well reproduced also by our simple model: (1) the ISIH (Fig. 4a) shows Gaussian shaped modes centered at integer multiples of the EOD period with a Gaussian envelope; (2) the return map (Fig. 4b) shows negatively sloped clusters as in the data; and (3) adjacent ISIs are negatively correlated (Fig. 4c). Our results are similar to those obtained in [3]. Note also that the model exhibits monotonically increasing tuning curves in agreement with experimental data [15] (Fig. 5).

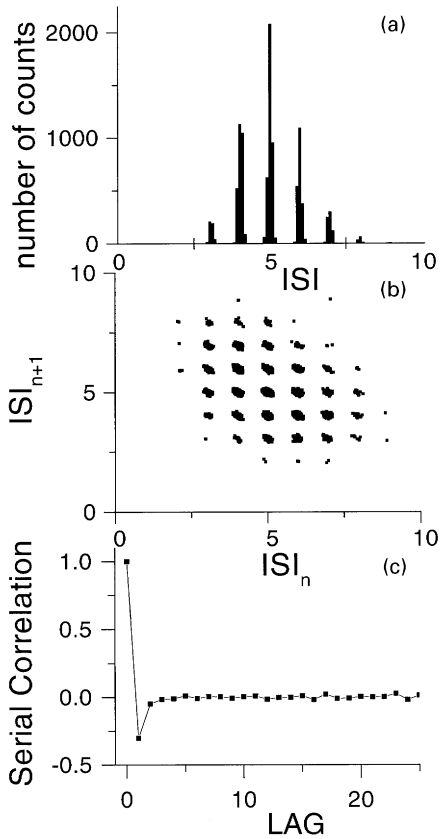

Fig. 4. Model firing statistics using 10 000 ISIs. (a) ISIH, (b) return map, (c) serial correlation. Parameters have the same values as in Fig. 3.

4. Extending the model to include bursting

We model bursting by incorporating a current that facilitates the occurrence of another spike following an action potential. Specifically, we introduce a delayed transient depolarizing current I_b that works as follows: after a spike has occurred, we wait for a time interval d after which it activates instantaneously and the onset of inactivation is modeled by exponential decay. The delay d may mimick the mean activation time of this transient current. I_b obeys the equation:

$$\dot{I}_b = -\frac{I_b}{\tau_b} + \Delta I_b \delta(t - t_{\text{fire}} - d). \tag{4}$$

Thus, we increment I_b by ΔI_b at time $t_{\text{fire}} + d$ (activation), and then allow exponential decay to zero (inactivation) with time constant τ_b until the next spike occurs. We now

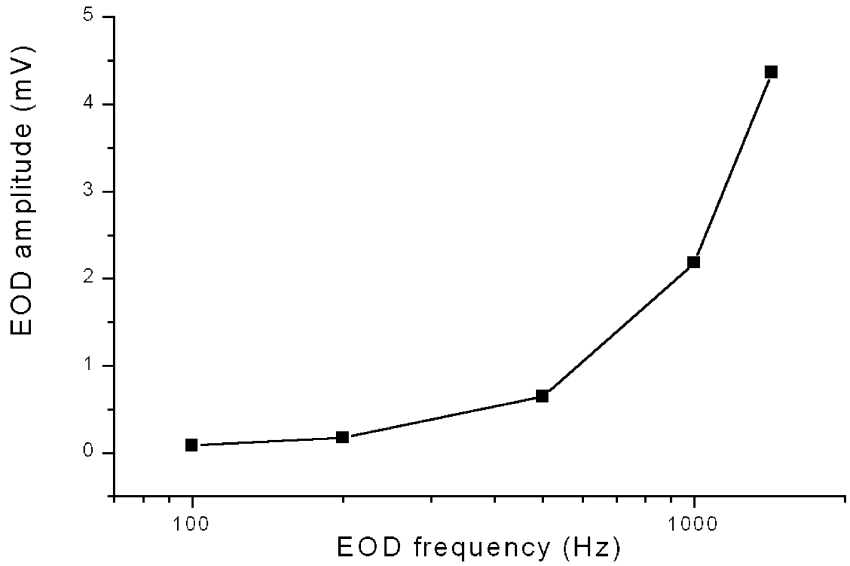

Fig. 5. Tuning curve obtained with the model. Each point is obtained by finding the lowest amplitude A giving rise to 1:1 firing for different EOD frequencies. Parameters have the same value as in Fig. 3.

take as input current the sum of I_{syn} in Eq. (3) and I_b in Eq. (4). Results obtained with periodic forcing and noise are shown in Fig. 6.

We can distinguish a burst (see arrow) consisting of three spikes fired on consecutive EOD cycles. The burst is initiated when θ is low and thus I_b can bring V to threshold on successive EOD cycles as seen by the series of sharp impulses. The threshold is higher after each action potential, and bursting thus terminates when θ is too high. Our model is thus based on the joint action of spike activated transient depolarizing currents and negative adaptation currents. These could be responsible for the intrinsic bursting behavior seen in such cells.

We show the results obtained with this model in Fig. 7 and compare them with the experimental data of Fig. 2. We see that the ISIH (Fig. 7a) has a prominent mode at one EOD period as in the data: the bursty P-unit thus tends to fire packets (bursts) of action potentials followed by quiescence as mentioned above. The return map (Fig. 7b) shows negatively sloped clusters as does the map for the data. Furthermore, we see that adjacent ISIs are negatively correlated (Fig. 7c).

In conclusion, this simple extension to our two-dimensional generic model of firing in non-bursty P-units exhibits, for a suitable choice of parameters values, the basic bursting properties seen experimentally.

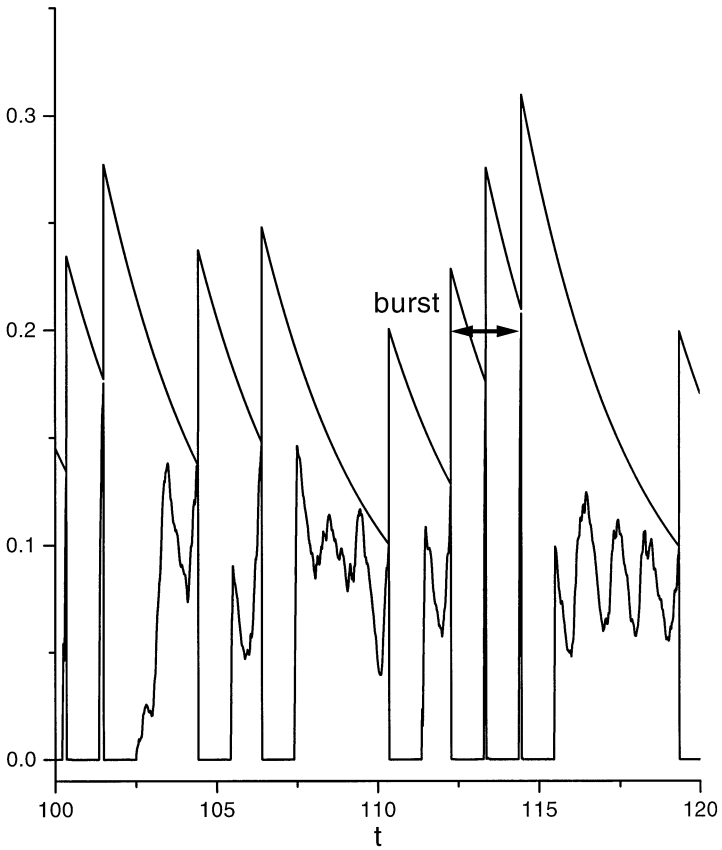

Fig. 6. Voltage (lower curve) and threshold (upper curve) trace obtained with the extended model (Eqs. (1)–(4)) exhibiting a bursting pattern. Parameters are the same as in Fig. 3 except: $\Delta\theta = 0.1$, $\tau_\theta = 4.7$, $D_1 = 19.531$, $D_2 = 0.328$, $d = 1$, $\Delta I_f = 1.4$, $\tau_f = 0.25$.

5. Discussion

We have presented models that reproduce the baseline firing characteristics for both bursting and non-bursting P-type electroreceptors of the weakly electric fish *Apteronotus Leptorhynchus*. The negative ISI correlations exhibited by the experimental data in both cases are a signature of refractoriness that persists for several EOD cycles. We have accounted for this in both cases by making the threshold vary with time and increasing the voltage-threshold distance immediately after a spike. This can model several physiological mechanisms [6,9,13]. Other models for adaptation [13,5] could also be combined with rectified periodic forcing to reproduce the data. However, the time constant of the refractory process is a key element of our model and underlies the approximately Gaussian envelope of the multimodal ISIH, a feature specific to electroreceptors.

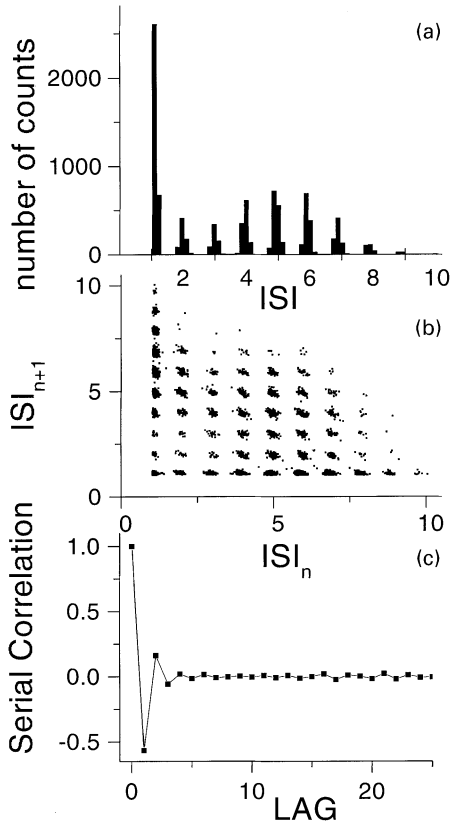

Fig. 7. Firing statistics of the extended model (Eqs. (1)–(4)) using 10 000 ISIs. (a) ISIH, (b) return map, (c) serial correlation. Parameters have the same value as in Fig. 6.

For both units, the dynamics are in the suprathreshold regime because periodic firing occurs in the absence of noise. The model predicts that the random skipping pattern seen experimentally results from noise added to the voltage dynamics. We obtain bursting by adding to the NB model a current that activates after a small delay following each action potential. The burst terminates when the threshold is too high and initiate again when it is low enough. Again, results from our extended model reproduce the experimental data. This shows that P-afferents can be modeled with a simple three variable system driven by noise. These models were designed to be computationally efficient while still reproducing the main features of the experimental data, since we are currently modeling population responses in the electrosensory periphery.

Acknowledgements

This work was supported by NSERC (M.J.C. and A.L.) and MRC (L.M.) Canada. We are grateful to N. Berman, J. Lewis, B. Doiron, P. Lánský, L. Schimansky-Geier, J. Freund and J. Milton for useful discussions, and to Mark Nelson (Beckmann Institute, Il). and Joe Bastian (U. Oklahoma at Norman) for sharing their data with us.

References

[1] J. Bastian, Electrolocation I. How the electroreceptors of Apteronotus Albifrons code for moving objects and other electrical stimuli, J. Comput. Physiol. A 144 (1981) 465.
[2] M.V.L. Bennett, C. Sandri, K. Akert, Fine Structure of the tuberous electroreceptor of the high-frequency electric fish *Sternachus albifrons* (gymnotiformes), J. Neurocytol. 18 (1989) 265.
[3] M.J. Chacron, A. Longtin, M St-Hilaire, L. Maler, Suprathreshold stochastic firing dynamics with memory in P-type electroreceptors, Phys. Rev. Lett. 85 (2000) 1573.
[4] A.S. French, A.V. Holden, R.B. Stein, The estimation of the frequency response function of a mechanoreceptor, Kybernetik 11 (1972) 15–23.
[5] C.D. Geisler, J.M. Goldberg, A stochastic model of the repetitive activity of neurons, Biophys. J. 6 (1966) 53–69.
[6] M. Hausser, A. Roth, Dendritic and somatic glutamate receptor channels in rat cerebellar Purkinje cells, J. Physiol. (Lond.) 501 (1997) 77–95.
[7] Y. Kashimori, M. Goto, T. Kambara, Model of P- and T-electroreceptors of weakly electric fish, Biophys. J. 70 (6) (1996) 2513–2526.
[8] A. Longtin, D.M. Racicot, Spike train patterning and forecastability, Biosystems 40 (1997) 111–118.
[9] T. Mickus, H.Y. Jung, N. Spruston, Properties of slow cumulative sodium channel inactivation in rat hippocampal CA1 pyramidal neurons, Biophys. J. 76 (1999) 846–860.
[10] M.E. Nelson, Z. Xu, J.R. Payne, Characterization and modeling of P-type electrosensory afferent responses to amplitude modulations in a wave-type electric fish, J. Comput. Physiol. A 181 (1997) 532–544.
[11] M.E. Nelson, M.A. MacIver, Prey capture in the weakly electric fish *Apteronotus Albifrons*: sensory acquisition strategies and electrosensory consequences, J. Exp. Biol. 202 (1999) 1195–1203.
[12] R.B. Stein, A theoretical analysis of neuronal variability, Biophys. J. 5 (1965) 173–194.
[13] A. Treves, Mean-field analysis of neuronal spike dynamics, Network 4 (1996) 259–284.
[14] Z. Xu, J.R. Payne, M.E. Nelson, Logarithmic time course of sensory adaptation in electrosensory afferent nerve fibers in a weakly electric fish, J. Neurophysiol. 96 (3) (1996) 2020–2032.
[15] H.H. Zakon, The electroreceptive periphery, in: T.H. Bullock, W. Heiligenberg (Eds.), Electroreception, Wiley, New York, 1986, pp. 103–105.

Maurice J. Chacron was born in Ottawa, Canada. He obtained a B.Sc. in physics Summa Cum Laudae at the University of Ottawa in 1998. He is now a Ph.D. student at the University of Ottawa under the supervision of Dr. André Longtin and Dr. Leonard Maler.

André Longtin is Associate Professor of Physics at the University of Ottawa. He completed is Physics B.Sc. in 1983, his M.Sc. (theoretical biophysics) in 1985 at the Université de Montréal, and his Ph.D. in Physics (non-linear dynamics) in 1989 at McGill University. He was an NSERC postdoctoral fellow in the Complex Systems Group and Center for Non-linear Studies at Los Alamos National Laboratory in 1989–1991. His main research interests lie in non-linear and stochastic dynamics, neuronal modeling and mathematical biology.

Leonard Maler obtained his B.Sc. from McGill University and his Ph.D. from the Massachussets Institute of Technology. Following PostDoctoral Fellowships at the Scripps Institute of Oceanography and the Max Planck Institute for Biophysical Chemistry, he accepted a position in the Faculty of Medicine at the University of Ottawa. Dr. Maler's research interests have focused on the role of feedback in sensory processing.